Mon. Not. R. Astron. Soc. **000**, 000–000 (0000) Printed 15 August 1997 (MN plain TEX macros v1.6)

X-ray selected active galactic nuclei with red optical continua

E. M. Puchnarewicz and K. O. Mason

Mullard Space Science Laboratory, University College London, Holmbury St. Mary, Dorking, Surrey RH5 6NT, UK.

ABSTRACT

We discuss the properties of X-ray selected 'red' AGN from the RIXOS sample. These are Seyfert 1 galaxies and quasars whose optical continua are relatively soft, i.e. with an energy index, $\alpha_{\rm opt}>2$. There are 14 objects in the RIXOS sample which satisfy this criterion and they cover a range in redshift from z=0.08 to 1.27. Of these, two have characteristics which suggest that the continuum is intrinsically red, i.e. an optical continuum which does not appear to have been significantly reddened by dust or to have contaminating light from the host galaxy. A further three objects show evidence of being absorbed by cold gas and dust with columns of up to $\sim 10^{22}$ cm^{-2}. The data are inconclusive on the remaining AGN.

Key words: Quasars: general – galaxies: active – galaxies: Seyfert – X-rays: general.

1 INTRODUCTION

The 'big blue bump' (BBB), a steep rise towards high frequencies in the optical/UV range, has been observed in many non-blazar AGN where it dominates the bolometric luminosity (e.g. Edelson & Malkan 1986; Elvis et al. 1994a). The apparent ubiquity of BBBs in AGN has justified the use of optical and UV-excess selection methods as an effective way of defining and identifying samples of AGN. However, deep optical observations of the blank fields around previously unidentified radio sources, have revealed a number of 'red' quasars (also termed 'optically-quiet' and 'optically-dull': see e.g. Rieke, Lebofsky & Kinman 1979; Ledden & O'Dell 1983; Bregman et al. 1985; Ulvestaad & Antonucci 1986; Elvis et al. 1994b; Kollgard et al. 1995). These quasars have unusually high radio-to-optical ratios and their colours suggest a steep, soft, IR-to-optical continuum slope.

Detailed studies of several of these objects have been made and in all cases the underlying cause of the red continuum is likely to be reddening by dust (e.g. Elvis et al. 1994b; Kollgard et al. 1995). Ledden & O'Dell (1983) found that optically-quiet radio sources also tended to be weak in X-rays and interpreted this as being due to the effects of absorption as well. These objects can provide us with some idea of the effects of dust on the overall quasar population, although even these may only represent a small minority of the reddened AGN population. This situation has major consequences for our interpretation of quasar properties, yet is notoriously difficult to tackle because of the problems in finding an unambiguous measurement of the amount of dust present (see e.g. Grandi 1983), and thus deriving the nature of the intrinsic AGN continuum.

A red continuum may have other explanations besides the presence of dust however. Two AGN with very strong EUV emission, RE J1034+396 and RE J1237+264 (Puchnarewicz et al. 1995; Brandt, Pounds & Fink 1995) have optical/UV continua which rise steeply to the red, yet their strong EUV/soft X-ray emission and low Balmer decrements argue against absorption. Similar properties are observed in the IR-selected IRAS13349+2438, although a *warm* (i.e. ionized), dusty absorber has been suggested for this AGN (Wills et al. 1992; Brandt, Fabian & Pounds 1996) and similar dusty warm absorbers have been inferred in the Seyfert galaxies MCG 6-30-15 (Reynolds et al. 1997) and NGC 3227 (Komossa & Fink 1997). Studies of RE J1034+396 have shown that the optical/UV continuum contained neither significant emission from the BBB nor from the host galaxy (Puchnarewicz et al. 1995), while the 2-10 keV *ASCA* spectrum (Pounds, Done & Osborne 1996) and *IRAS* 12-100μm colours are consistent with an extrapolation of the optical/UV slope to higher and lower energies. In addition, the optical spectrum does not exhibit any linear polarization, with an upper limit of ∼0.3-0.4 per cent (Breeveld & Puchnarewicz 1997). All of this evidence points to an *intrinsically* red optical/UV slope in RE J1034+396, which is part of an underlying power-law component and extends from 100μm to 10 keV.

Objects like these and the radio-selected red quasars have led authors to comment on their similarity to blazars and speculate on a possible link between these and non-blazar AGN (e.g. Rieke et al. 1979; Bregman et al. 1985; Puchnarewicz et al. 1995; Tananbaum et al. 1997). The existence of IR to X-ray power-law continua in non-blazars has been disputed however; while observations indicate that such a component may be common in AGN (Malkan 1984; Elvis et al. 1986), it has been demonstrated that such effects may be mimicked by the sum of several thermal components (e.g. Barvainis 1993). If a power-law component could be confirmed, it would have implications for non-thermal emission mechanisms in AGN and for the relationship between AGN and blazars.

Both types of red AGN, i.e. intrinsically-red objects and dust-reddened sources, will have been selected against when UV-excess techniques are used to search for and identify AGN. Previous identifications of red AGN have largely been made by means of the optical identification of radio sources (e.g. Rieke et al. 1979; Bregman et al. 1985). Kollgard et al. (1995) used the *ROSAT* All-Sky Survey to search for their 'optically-quiet' quasars, although radio-loudness was a defining criterion in their study. In this paper, we have used the X-ray (0.5-2 keV) selected RIXOS sample of AGN (Mason et al. , in preparation) to investigate the incidence of red AGN, independent of their radio loudness. The properties of the RIXOS AGN sample as a whole are presented in Puchnarewicz et al. (1996; the continua, hereafter Paper I) and Puchnarewicz et al. (1997; emission lines, hereafter Paper II).

While selection in any restricted wavelength range is not perfect, the advantages of using the RIXOS sample for the study of red AGN are *(1)* that it reaches X-ray fluxes typically 10 times fainter than the EMSS (Gioia et al. 1990; Stocke et al. 1991); and *(2)* UV-excess was *not* a determining factor when an AGN identification was made. Thus these AGN can suffer a greater degree of cold gas absorption before they become too faint to detect, providing a wider range of absorbing columns, and AGN with red optical slopes would not have been discriminated against. This sample provides an essential comparison between radio-selected and X-ray-selected red AGN. We investigate the nature of any absorption and the possibility that the optical slope may be a bare, intrinsically red power-law continuum with no BBB (at least down to the near-UV). Finally, the implications of these results on the nature of AGN emission processes and on population studies of AGN are discussed.

2 DATA REDUCTION

2.1 The RIXOS AGN and the red subsample

The RIXOS sample (Mason et al. in preparation) is made up of objects discovered serendipitously in medium deep (exposure >8 ksec), high Galactic latitude ($|b| > 28°$) pointed observations made with the *ROSAT* Position Sensitive Proportional Counter (PSPC; Pfefferman et al. 1986). Only sources within 17 arcmin of the centre of the field and with a flux greater than 3×10^{-14} erg cm^{-2} sec^{-1} in the *ROSAT* 'hard' band (0.4-2.0 keV) are used; optical identification of survey sources is 94 per cent complete to this flux level over 15 deg^2. This has produced a sample of X-ray emitting AGN (i.e. Seyfert 1s to 1.9s and quasars), selected irrespective of the strength or shape of the optical/UV continuum. There are 160 objects in this RIXOS subsample with unambiguous redshifted line emission and broad permitted line widths [i.e. with full widths at half maximum (FWHM) of 1000 km s^{-1} or more; see Paper II].

2.1.1 *Measuring the optical continuum slope*

Optical spectral indices, $\alpha_{\rm opt}$, have been measured for 145 of these AGN by fitting a simple power-law to the data, having first removed all absorption and emission features and regions with a very low signal-to-noise ratio. For the remaining 15 objects, either no spectrum was available [because the source had been previously identified and the optical slope was not available in the literature (6 sources)], or the spectrum was not taken with the slit at the parallactic angle (9 sources). Although Balmer continuum and optical FeII emission can blend to produce a "quasi"-continuum at around 3000 Å (Wills, Netzer & Wills 1985) which may affect measurements of $\alpha_{\rm opt}$, this has been reduced by removing these features and by using the broadest wavelength range available (∼5000 Å in the observer-frame). Full details of the optical observations and derivations of the optical power-law slopes may be found in Paper II.

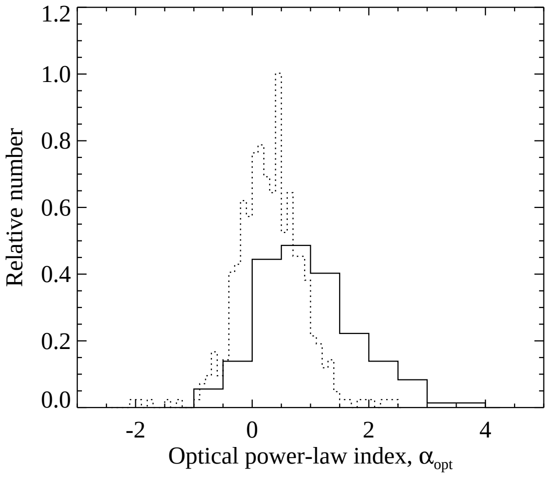

Figure 1. The distribution of optical power-law indices, $\alpha_{\rm opt}$, for the RIXOS AGN (plotted as a solid line) and compared with the bright quasars from the Francis et al. (1991) sample (dotted line). Both distributions have been normalized by area.

Errors on the optical slopes are dominated by systematics and are difficult to determine for individual spectra. We have assessed the typical error expected on the slopes from the dispersion in the measured values for sources from the parent sample which were observed more than once and estimate that the uncertainty in $\alpha_{\rm opt}$ is conservatively $\sim \pm0.5$.

2.1.2 *Red sample selection*

The distribution of $\alpha_{\rm opt}$ for the RIXOS AGN is shown in Figure 1 ($\alpha_{\rm opt}$ and all indices α are defined such that $F_\nu \propto \nu^{-\alpha}$). The mean $\alpha_{\rm opt}$ is 0.9±0.1 (the error quoted is the error on the mean), which is softer than typical median values for UV-excess selected quasars where $\alpha_{\rm opt}$∼0.2-0.3 (e.g. Neugebauer et al. 1987; Francis et al. 1991). The distribution of the Francis et al. (1991) sample is compared with the RIXOS AGN in Fig 1. This illustrates the tendency for the X-ray selected RIXOS objects to have softer optical slopes than optically-selected AGN and suggests that a significant population of 'red AGN' may be missing from optically-selected samples.

For the purposes of this study, we have (arbitrarily) chosen $\alpha_{\rm opt}\geq2$ as the definition of a 'red' AGN. This selects the 14 softest AGN from the RIXOS sample; the softest 10 per-cent of objects. They are also very soft when compared to optically-selected quasars, e.g. in the Francis et al. (1991) sample shown in Fig. 1, only 4 of the 419 quasars had $\alpha_{\rm opt}\geq2$. The RIXOS red AGN source list including redshifts, J2000 positions, spectral V-band magnitudes and $\alpha_{\rm opt}$ are given in Table 1.

Table 1. RIXOS red AGN source list

FID	SNo	z	RA (J2000)	Dec (J2000)	m_V	α_{opt}	α_{ox}	α_{ro}	α_{rx}
122	13	0.358	16 30 55.10	+78 11 02.0	20.6	3.1	1.0	<0.4	<0.5
122	21	0.376	16 34 27.80	+78 10 03.0	20.8	2.3	1.0	<0.4	<0.5
218	14	0.224	09 52 50.30	+ 7 50 34.6	20.9	2.6	0.9	—	—
219	45	1.272	12 54 56.70	+56 49 41.0	21.9	2.4	0.8	<0.5	<0.6
220	23	0.193	17 26 19.27	+74 48 01.9	19.9	3.8	1.3	<0.3	<0.7
223	17	0.288	16 33 09.60	+57 10 40.0	19.3	2.1	1.2	—	—
232	16	0.227	10 08 58.82	+50 37 30.7	19.9	2.2	1.2	<0.3	<0.6
248	2	0.274	09 09 43.56	+43 02 54.6	21.9	2.4	0.9	<0.5	<0.6
255	7	0.260	07 59 06.74	+37 32 35.9	21.2	2.6	1.2	<0.4	<0.7
258	1	0.698	11 17 50.71	+07 57 11.9	21.5	2.4	0.4	—	—
273	23	0.433	10 42 50.30	+11 51 19.0	20.6	2.3	1.3	—	—
278	10	0.091	13 31 52.15	+11 16 49.8	16.7	3.0	1.2	<0.1	<0.5
281	21	0.347	00 10 33.51	+10 52 31.3	20.2	2.4	1.1	<0.3	<0.6
293	13	0.189	08 20 12.69	+37 35 02.8	21.6	2.6	0.9	<0.4	<0.5

FID: RIXOS field number; SNo: RIXOS source number; z: AGN redshift; RA and Dec: position of the optical counterpart in J2000; m_V: apparent V band magnitude measured from the optical spectra; α_{opt}: energy index of the best-fitting power-law to the optical continuum; α_{ox}: energy index of slope connecting 5000 Å to 2 keV; α_{ro}: energy index of slope connecting 1.4 GHz to 5000 Å; α_{rx}: energy index of slope connecting 1.4GHz to 2 keV.

2.2 Analysis of the X-ray data

As part of the original survey analysis, the PSPC data for all AGN were divided into three bands [0.1 to 0.4 keV (channels 8 to 41); 0.5 to 0.9 keV (channels 52 to 90) and 0.9 to 2.0 keV (channels 91 to 201)] and these were combined to produce 'spectra' with three data points for each source. The spectra were fitted with single power-law models using the method described in Mittaz et al. (1997), which finds the best-fit by minimizing a Poissonian-based statistic. In the fits, the absorbing column density was fixed at the Galactic column ($N_{\rm HGal}$) measured from the 21 cm survey of Stark et al. (1992). All instrumental effects, including vignetting, dead-time corrections and particle contamination, were folded into the fitting process. The data were also corrected for any counts falling outside the extraction circle. These are subsequently referred to as the 'three-colour' data.

For this study, we have also extracted the full-resolution PSPC spectra of those sources which have a total of at least 100 net counts; seven of the 14 sources fall into this category. Using the standard ASTERIX software, the source spectra were extracted using circles with radii of up to 2.5 arcmin (depending on the position of any adjacent sources) and a nearby source-free region was used for background subtraction. Counts were binned to yield at least 20 per energy bin, ignoring channels 1-11 (channels 1-8 for data taken before the PSPC detector was changed in January 1991) and channels 201-256 where the response is uncertain. The spectra have been corrected for all instrumental effects including vignetting, dead-time and particle contamination.

The reduced PSPC data were fitted using the XSPEC spectral fitting software. The Galactic column density in the direction of each source ($N_{\rm HGal}$) was calculated by interpolating between the 21 cm measurements of Stark et al. (1992). A single power-law model was fitted to each spectrum with a cold absorbing column fixed at the Galactic value, allowing the index and normalization of the power-law to be free parameters. In all cases, these power-law models provided a good fit to the data with $\chi^2_\nu \sim$1 (see Table 2a).

A second fit was performed with an additional cold absorption column which was redshifted into the rest-frame of the quasar and whose column density ($N_{\rm Hint}$) was allowed to be a free parameter (i.e. giving 3 free parameters). However, no significant improvements to the fits (according to the F-test) were found to any of the AGN and only 90 percent upper limits could be derived on $N_{\rm Hint}$ (these are given in Table 3). The constraints on two AGN, F223_17 and F248_2, are relatively tight however, with 90 percent upper limits of 2×10^{20} cm^{-2} and 3×10^{20} cm^{-2} respectively, indicating low levels of cold gas absorption in these objects.

For those AGN with too few counts for full spectral fitting, the fits to the three-colour data (with 90 percent errors) from Mittaz et al. (1997) are given in Table 2b. Slopes derived from the three-colour data are also listed for the objects with full-resolution PSPC data for comparison (see Table 2a); the two sets of slopes are consistent within the 90 per cent errors.

2.3 Radio fluxes

We have searched for evidence of radio activity in the red AGN using the NRAO/VLA Sky Survey (NVSS; Condon et al. , in preparation). The NVSS covers the sky north of –40° at a frequency of 1.4 GHz to a limiting peak source brightness of about 2.5 mJy. At the time of writing, sky coverage was available for ten of the 14 AGN, although none were detected. Using 2.5 mJy as an upper limit on the radio brightness, we have calculated upper limits on the radio-to-optical and radio-to-X-ray indices (α_{ro} and α_{rx} respectively) for these ten sources, and these are listed in Table 1.

Table 2a. Results of X-ray spectral fitting

FID	SNo	z	radius arcmin	$N_{\rm HGal}$ 10^{21} cm^{-2}	Model with $N_{\rm H}$=$N_{\rm HGal}$ $\alpha_{\rm x}$	norm	χ^2/dof	Mittaz et al. $\alpha_{\rm x}$
122	13	0.358	0.4	0.41	$-0.1^{+0.3}_{-0.4}$	3.4	5/9	$0.0^{+0.5}_{-0.7}$
122	21	0.376	2.5	0.41	$-0.3^{+0.6}_{-0.7}$	2.7	5/5	$0.2^{+0.5}_{-0.7}$
219	45	1.272	0.4	0.13	$0.6^{+0.2}_{-0.2}$	3.2	12/9	$0.6^{+0.3}_{-0.3}$
223	17	0.288	2.5	0.18	$1.5^{+0.1}_{-0.1}$	6.6	54/49	$1.4^{+0.1}_{-0.1}$
248	2	0.274	1.0	0.15	$0.9^{+0.2}_{-0.2}$	3.5	11/11	$0.8^{+0.2}_{-0.2}$
258	1	0.698	2.5	0.34	$0.3^{+0.4}_{-0.6}$	7.2	6/6	$-0.2^{+0.5}_{-0.6}$
278	10	0.091	2.5	0.19	$-1.2^{+0.4}_{-0.4}$	18.2	13/15	$-1.6^{+0.6}_{-0.7}$

FID: RIXOS field number; SNo: RIXOS source number; z: AGN redshift; $N_{\rm HGal}$: Galactic absorbing column density in units of 10^{21} cm^{-2}; radius: the radius of the circle used to extract the X-ray spectrum in arcminutes; $\alpha_{\rm x}$: energy index of the best-fitting power-law model; norm: normalization of the best-fitting power-law in units of photon 10^{-5} keV^{-1} cm^{-2} s^{-1} at 1 keV; χ^2/dof: chi-squared per degrees of freedom of the fit. All errors shown in the table are 90 percent. Errors on $N_{\rm HGal}$ are ∼10 percent.

Table 2b: Fits to three-colour data

FID	SNo	z	$N_{\rm HGal}$ 10^{21} cm^{-2}	Mittaz et al. $\alpha_{\rm x}$	norm
218	14	0.224	0.30	$1.1^{+0.6}_{-0.5}$	3.8
220	23	0.193	0.39	$-0.2^{+1.4}_{-3.0}$	2.5
232	16	0.227	0.08	$0.7^{+0.5}_{-0.6}$	1.4
255	7	0.260	0.51	$1.3^{+1.1}_{-2.9}$	1.6
273	23	0.433	0.28	2.3^{u}	1.3
281	21	0.347	0.58	$0.7^{+0.9}_{-1.4}$	3.7
293	13	0.189	0.46	$0.3^{+1.1}_{-1.9}$	3.3

Details as for Table 2a. All errors shown in the table are 90 percent; errors for F273_23 are not given because the fits to the three-colour data were poorly determined. Errors on $N_{\rm HGal}$ are ∼10 percent.

3 ANALYSIS AND RESULTS

The optical-to-X-ray continua of the red RIXOS AGN are shown in Figure 2 to illustrate the X-ray spectra relative to the optical, and the overall shape for each individual AGN. All of the AGN in this study have a Galactic $N_{\rm H}$ which is relatively low and does not itself significantly modify the intrinsic spectrum. The continuum may look red in the optical for several reasons: *1.* dust absorption, which is wavelength-dependent and preferentially removes the blue photons; *2.* a contribution from the host galaxy, which is strongest in the red part of the spectrum; and *3.* an intrinsically red continuum produced by the nucleus and unmodified along our line of sight. Sources which do not show evidence for absorption or a strong galactic contribution are presumed to have an intrinsically red optical slope.

3.1 Absorbed sources

Supporting evidence for absorption, apart from the optical continuum slope, may be found from two main sources, the Hα/Hβ flux ratio (i.e. the Balmer decrement) and the level of cold gas absorption local to the AGN. If case B recombination is appropriate for the BLRs in AGN, then the Balmer decrement in *un*absorbed AGN should be ∼3. Thus we first look for a high Hα/Hβ flux ratio as evidence of dust absorption.

The effects of absorption may also be seen in soft X-rays. The optical continuum can only be reddened by optically-thin dust dominated by small grains (Laor & Draine 1993), and since this can only exist at relatively large distances from the centre, we assume that the dust probably resides in cold gas. Therefore a measurement of a significant cold gas column from the PSPC data would also suggest that a large dust column may be present, although the presence of dust-free gas cannot be ruled out. Dust in warm gas has been inferred in some nearby Seyferts (Brandt et al. 1996; Komossa & Fink 1997; Reynolds et al. 1997), however the resolution and overall quality of the PSPC data used for the red RIXOS AGN are not sufficient to distinguish possible columns of warm gas.

3.1.1 Balmer decrement

The Balmer decrement has been measured for three AGN and upper limits have been calculated for a further five. Errors on the Balmer decrements have been derived by estimating upper and lower limits on the Balmer line fluxes, taking into account the placement of the continuum and other effects such as line blending and the relative contribution of the narrow component. The results are listed in Table 3 and show that for all but two AGN, F232_16 and F281_21, the Balmer decrement is high, suggesting significant amounts of intrinsic dust absorption. The degree of extinction by dust, parametrized by E(B-V), has been calculated from these Balmer decrements using the reddening curve of Cardelli, Clayton & Mathis (1989), and these are also given in Table 3 (column 5).

If it can be assumed that differences in the Balmer decrement are entirely due to reddening by dust, then it should be possible to use the Hα/Hβ flux ratio to predict the intrinsic (i.e. unreddened) optical continuum slope using reddening curves which have been derived for the dust

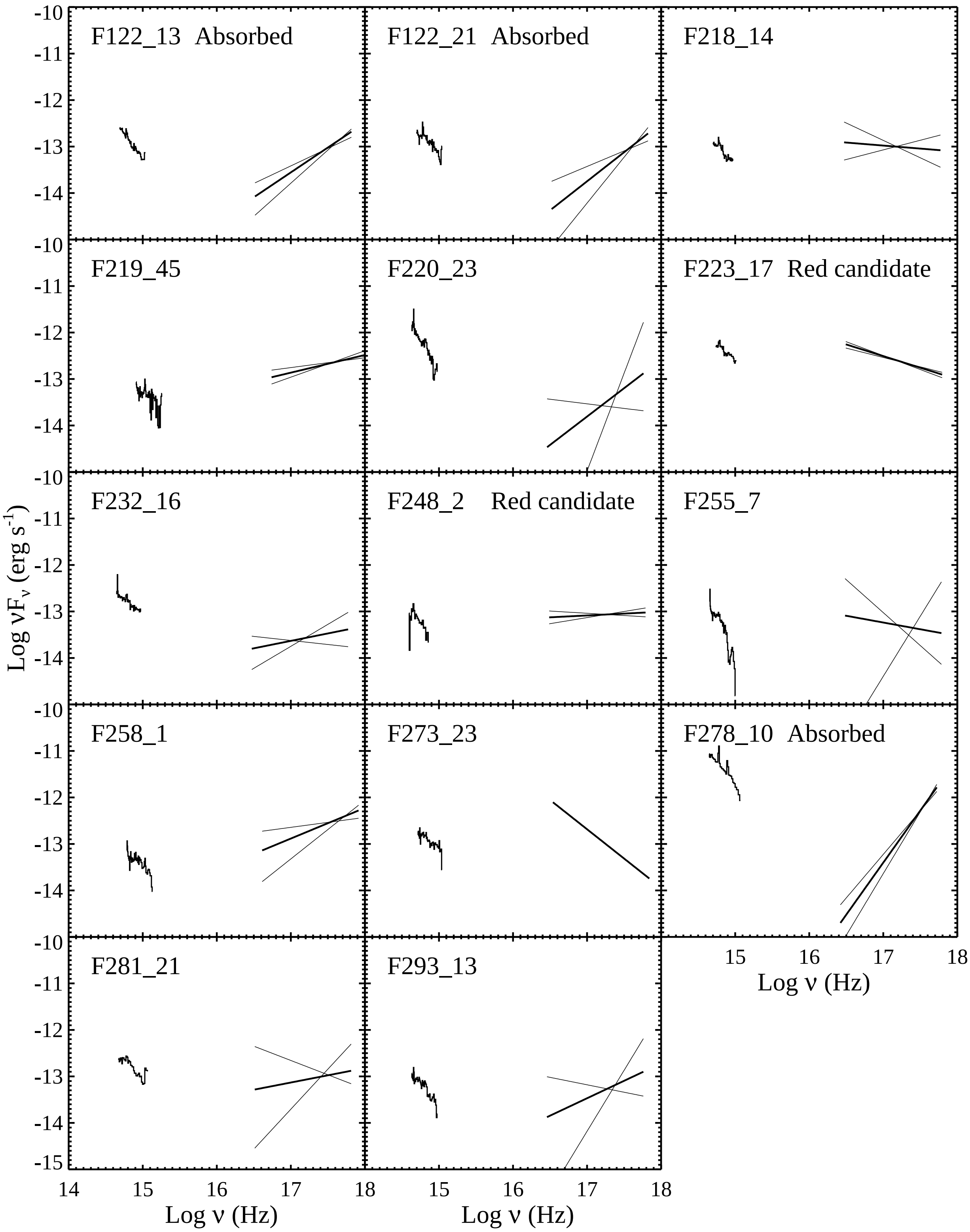

Figure 2. Multiwavelength spectra for the red AGN. All spectra are plotted in the AGN rest-frames.

Table 3. Absorbing columns and intrinsic optical slopes

FID	SNo	cold gas	dust extinction		intrinsic $\alpha_{\rm opt}$	
		$N_{\rm Hint}$ 10^{21} cm^{-2}	Hα/Hβ	E(B-V)	($N_{\rm Hint}$)	(Hα/Hβ)
(1)	*(2)*	*(3)*	*(4)*	*(5)*	*(6)*	*(7)*
122	13	<7.6			>-1.7	
122	21	<25			>-10	
218	14		9 (2,17)	0.9 (0,1.4)		-0.5 (-2.7,2.6)
219	45	<3.6			>-0.4	
220	23		>4	>0.1		<3.5
223	17	<0.2			>2.0	
232	16		4 (2,11)	0.2 (0,1.1)		1.3 (-2.0,2.2)
248	2	<0.3	>2.3	>0.0	>2.2	<2.4
255	7		>6.1	>0.6		<0.5
258	1	<14			>-7.1	
278	10	<18	>7	>0.7	>-7.2	<-0.2
281	21		2 (1,26)	0 (0,1.8)		<2.4
293	13		>1.2	>0.0		<2.6

(1): RIXOS field number; *(2)*: RIXOS source number; *(3)*: 90 percent upper limit on the intrinsic cold absorption column density from X-ray spectra in units of 10^{21} sm^{-2}; *(4)*: Balmer decrement measured from the optical spectrum (lower and upper limits); *(5)* dust extinction implied by Balmer decrement using reddening curve of Cardelli et al. (1989) (lower and upper limits); *(6)* hard (lower) limit on the energy index of the intrinsic optical continuum derived from 90 percent upper limits on the X-ray absorbing column $N_{\rm Hint}$ (Section 3.1.2); *(7)* energy index (errors in brackets) of the intrinsic optical continuum calculated using the Balmer decrement (Section 3.1.1).

in our Galaxy. This was done for the red AGN by first dereddening the spectrum using the Cardelli et al. (1989) data and then fitting a power-law to the resultant spectrum; the derived intrinsic $\alpha_{\rm opt}$ (with errors calculated from the errors on the Balmer decrement) is given in column 7 of Table 3.

The table shows that due to the low signal-to-noise of the RIXOS optical spectra and subsequently the large errors on the Balmer decrement, values for the intrinsic (i.e. the dereddened) $\alpha_{\rm opt}$ are poorly constrained and in most cases, no firm conclusions can be drawn. Sources F278_10 and F255_7 have dereddened optical spectra which are no longer 'red' (the dereddened $\alpha_{\rm opt}$ is significantly lower than 2), i.e. their intrinsic optical continua are relatively hard and typical of UV-selected quasars (under the assumptions of this method). All other objects have upper limits which are greater than 2, i.e. their intrinsic optical continua may be red. None of the AGN have a dereddened $\alpha_{\rm opt}$ which remains significantly red (i.e. $\alpha_{\rm opt}>2$).

3.1.2 *Cold gas columns from X-ray spectra*

Fits to the full-resolution *ROSAT* PSPC spectra show that for two out of the seven objects, F223_17 and F248_2, the best-fit $N_{\rm Hint}$ was low (with 90 percent upper limits of 2 and 3×10^{20} cm^{-2}), implying very little cold gas absorption in these AGN (although the possibility of *warm* absorption cannot be ruled out; see Section 3.1). Column densities on the remaining five AGN are poorly constrained; intrinsic cold gas column densities of up to 3×10^{22} cm^{-2} are possible (90 percent upper limits).

While they do not provide measurements of any cold gas column, the upper limits on $N_{\rm Hint}$ can be used to assess whether sources are likely to be intrinsically red. By assuming that any cold absorbing gas carries a given amount of dust, the upper limits on $N_{\rm Hint}$ may be used as an indication of upper limits on the amount of *dust* along the line of sight. The intrinsic $\alpha_{\rm opt}$ may then be derived using a method similar to that described in section 3.1.1. Limits on E(B-V) have been calculated from the limits on $N_{\rm Hint}$ (Table 3) using a Galactic dust-to-gas ratio, where an E(B-V) of 1 corresponds to $N_{\rm H}=6\times10^{21}$ cm^{-2} (Ryter, Cesarsky & Audouze 1975; Gorenstein 1975). This dust extinction was then used to calculate a *lower* limit on the intrinsic slope of the optical continuum.

The results are listed in Table 3 and show that in most cases, the lower limits on the de-reddened $\alpha_{\rm opt}$ are very low and little useful information can be derived. However, two of the seven AGN have optical continua which do remain red, F223_17 and F248_2, thus we identify these as 'red candidate' AGN, i.e. those whose optical continua does not appear to have been significantly modified by dust or the host galaxy.

3.1.3 *Galactic contamination*

No features similar to that of a typical underlying host galaxy (e.g. Ca H and K lines, and NaD at 5893 Å) could be found in any of the low-z AGN (i.e. with $z\leq0.5$). The optical spectra of AGN at higher redshifts cover shorter wavelengths in the rest-frame where any galactic contribution is relatively weak. Thus the host galaxy is unlikely to cause the reddening of the optical continuum of objects in this sample.

3.2 Red candidates

We find that, of the 14 RIXOS AGN with an $\alpha_{\rm opt}>2$, two (the 'red candidates'; F223_17 and F248_2) have an optical

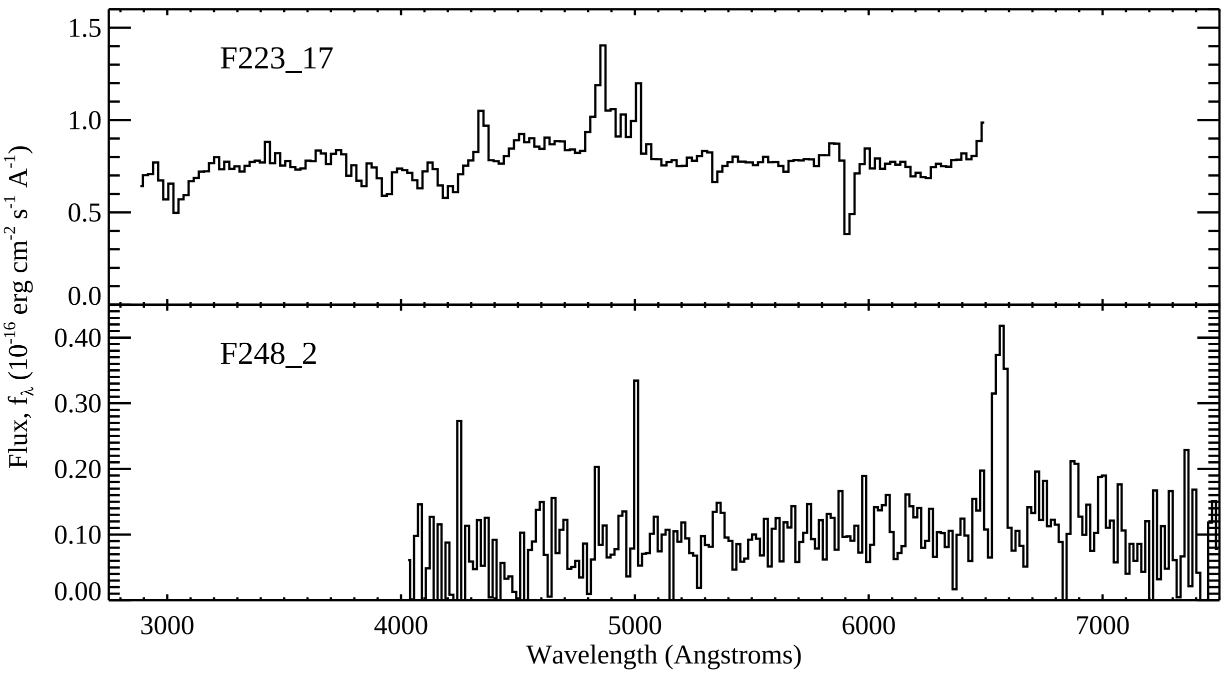

Figure 3. The optical spectra for the red AGN candidates (see Section 3.2). Both spectra are plotted in the rest-frames of the AGN and have been binned up to a resolution of ∼20 Å per bin for clarity.

continuum which remains red by this definition, even after correction for any dust absorption by the methods outlined in Section 3.1. Optical spectra of the red candidate AGN are plotted in Figure 3.

The red candidates are a particularly interesting group because of the implications they present for models of a possible underlying optical power-law continuum in AGN, as well as for the use of optical/UV-selected samples as representative populations of Seyferts and quasars. Thus, to search for any evidence of other systematic differences which might provide further clues to their physical nature, we compared their continuum (luminosities at 5000 Å, 2500 Å and 2 keV from Paper I) and line emission properties (Hα, Hβ and [OIII] equivalent widths and full widths at half maximum from Paper II) with the rest of the RIXOS AGN. However, we could find no significant differences between the properties of the red candidates and the parent sample.

3.3 Absorbed AGN

For the remaining 12 AGN, some degree of absorption by dust is a possible explanation for the reddening of the optical continuum. However, quantifying the dust column is not a straightforward task. In Section 3.1, we showed that the dust and cold gas columns derived from the available data are poorly constrained in many cases, due to the relatively poor quality of the optical and *ROSAT*-PSPC spectra.

Nonetheless, an indication of whether significant absorption might be occurring in a source can be derived from the slope of the X-ray spectrum which was calculated assuming a fixed Galactic $N_{\rm H}$ (i.e. $N_{\rm H}$=$N_{\rm HGal}$; see, eg., Fig. 2). This slope describes the shape of the AGN's X-ray spectrum extrinsic to our Galaxy, and reflects how the nuclear continuum may have been modified by gas along the line of sight. Studies of Seyferts and quasars (e.g. Walter & Fink 1993; Laor et al. 1997; Boyle, Wilkes & Elvis 1997) have shown that intrinsic slopes in the PSPC band, $\alpha_{\rm x}$, range between ∼1.3 and 1.6, and for RIXOS, the mean $\alpha_{\rm x}\sim1$ (Paper I; Mittaz et al. 1997); at higher energies the typical $\alpha_{\rm x}$ is also ∼1 (e.g. Comastri et al. 1992). Thus we assume that any AGN with a relatively hard $\alpha_{\rm x}$, i.e. $\alpha_{\rm x}<0.5$, suffers cold gas absorption external to our Galaxy. Adopting this limit and taking into account the 90 percent errors, we find that three of the red RIXOS AGN are likely to be absorbed by cold gas (F122_13, F122_21 and F278_10), thus their optical continua have probably been absorbed by dust.

4 DISCUSSION

The very existence of AGN with red IR/optical/UV slopes has an impact on many areas of AGN research. The proliferation of BBBs in optical and UV spectra has naturally led to the presumption that most, if not all, AGN have such a component. Looking for sources with a strong blue excess in optical wavelengths is a common method used for identifying AGN; by using the presence of a blue optical continuum as an initial defining criterion, the apparent domination of blue sources is maintained. However, the models of AGN structure which are currently popular have significant covering factors of dust and gas, thus large numbers of reddened sources should be expected. Furthermore, EUV-selected AGN with red optical continua already present strong evidence for intrinsically red objects. We discuss our analysis of these X-ray selected red AGN, the implications of a large 'hidden' population of reddened quasars and the possibility of a new class of 'intrinsically red' Seyferts and quasars.

4.1 Radio properties of red AGN

Most of the red quasars identified previous to this study, have been discovered in radio samples and thus most (if not all) have been radio-loud. This has led to speculation that radio loudness may in fact be a requirement for a red quasar (Elvis et al. 1994b). Of the ten sources in the RIXOS red AGN sample for which radio data were available, none were found to be significant radio emitters. We thus conclude that radio loudness is not a necessary condition for red AGN. It is more likely that the apparent trend for the red quasars to be strong radio sources is due to their selection from radio surveys.

4.2 The effects of absorption

Along our line of sight to any quasar nucleus, there are many possible sites for dust (external to our Galaxy), e.g. in the outer regions of the nucleus itself, in the quasar's host galaxy, and in any intervening galaxies. The covering factor of the dusty molecular torus alone is estimated to be $\sim$0.4 (Krolik & Begelman 1986). It might seem surprising then, that we have a relatively 'clean' line of sight to so many AGN and that the overall population is *not* dominated by reddened sources. Webster et al. (1995) have made an estimate of the 'missing' red sources and find that as many as 80 percent of radio-quiet AGN may be overlooked in optical/UV-selected samples.

Assuming that the dust resides in cold gas, then soft X-ray-based samples will suffer from similar selection problems because the soft X-rays are very readily absorbed by the gas, especially below $\sim$0.5 keV. The RIXOS AGN were selected by their 0.5-2 keV flux to a limit of 3×10^{-14} erg cm^{-2} s^{-1}. These criteria have allowed AGN with a greater range of absorbing columns at fainter fluxes to be detected which is beneficial when searching for objects which moderate amounts of reddening ($N_{\rm Hint}$ of up to a few times 10^{21} cm^{-2}). In Paper I, we placed a lower limit of $\sim$0.3 on the fraction of AGN which have significant gas and dust columns (i.e. with $N_{\rm Hint}\gtrsim 10^{21}$ cm^{-2}), i.e. we find that *at least* a third of AGN have moderate to large absorbing columns.

In this paper, we have highlighted the reddest of the RIXOS AGN, i.e. those with an $\alpha_{\rm opt}>2$. Fourteen of the 160 RIXOS AGN meet this criterion and of these, three show positive evidence of absorption, based on the slope of the X-ray spectrum extrinsic to our Galaxy (see, eg., Figure 2). Modelling of the X-ray spectra has shown that equivalent intrinsic cold gas columns of up to 10^{22} cm^{-2} are possible. This is small compared to the expected column density of the dusty molecular torus however ($\sim 10^{24}$ cm^{-2}; Krolik & Begelman 1988); if such large columns are typical of AGN in general then it should indeed be anticipated that many AGN are being missed.

The consequences of using a select group of relatively unabsorbed objects to represent the properties of a much larger, mixed population of AGN are difficult to assess. If, as suggested by the 'unified model' (see e.g. Antonucci 1993 for a review), the observed properties of an AGN are largely determined by the orientation of the molecular torus, this presumption is valid *unless* there are other angular-dependent properties in the inner regions. For example, if emission from an accretion disc is angular dependent (e.g. Sun & Malkan 1989; Czerny & Elvis 1987; Madau 1988) and the disc is co-aligned with the torus, only the disc's properties at relatively face-on angles can be observed. In Paper II however, we found that angular-dependence may not accurately reflect the amount of dust present, in which case there may be more fundamental implications for the 'hidden' population, e.g. the amount of obscuring dust and gas may be related to the intrinsic source luminosity, black hole mass and/or host galaxy type; it is only possible to speculate at this stage.

4.3 Unabsorbed red AGN

Out of the 14 AGN studied, two show convincing evidence for little or no absorption and are probably 'intrinsically' red. These objects have low cold gas columns and in general their X-ray emission lies well above an extrapolation of the optical continuum. There is *no* BBB emission in these sources down to wavelengths of $\sim$3000 Å; other reports of AGN with weak optical BBBs have also been made (e.g. McDowell et al. 1989). The intrinsically red RIXOS AGN may be similar to some EUV-bright Seyferts whose BBBs are so hot that they are not observed even in the UV, but are unusually strong in the EUV and soft X-rays, even showing evidence of a high-energy turnover at $\sim$1 keV (e.g. Puchnarewicz et al. 1995). F223_17 is the most likely analogue of these. Alternatively the BBB may be emitted away from our line of sight, or entirely suppressed.

Another important question posed by the intrinsically red sources is the nature of the optical continuum itself. There are two components which are known to be strong in the optical range, the BBB and the host galaxy, yet there is evidence for neither in these AGN. What, then, is the origin of the red, continuum component which is observed? The resemblance of the radio to optical spectra of 'red' or 'optically-quiet' radio sources to blazars (e.g. Rieke et al. 1979; Ledden & O'Dell 1983; Tananbaum et al. 1997) is intriguing and there may be some relationship between the two. From a different approach, Ulvestaad & Antonucci (1986) examined three BL Lacs in greater detail and suggested that, if seen from a less pole-on direction, these would probably be classified as 'optically-dull' radio galaxies. Perhaps the red quasars are blazars seen close enough along the jet axis that the blazar continuum is observed, but not strong enough to swamp the emission lines.

Tananbaum et al. (1997) have suggested that there may be a physical link between the radio emission and the relatively low optical emission in the galaxy J 2310–43, based on the model of Donea & Biermann (1996), where optical/UV emission from an accretion disc is suppressed when the base of the radio jet is large. The intrinsically red AGN are all radio-quiet however, thus an unusually large radio jet is unlikely to be the cause of the red optical/UV continuum.

5 CONCLUSIONS

We have presented a study of 14 'red AGN' from the RIXOS sample. The sources all have relatively soft optical continuum slopes, with an $\alpha_{\rm opt}>2$. Of the ten for which radio data are available, all are radio-quiet. At least two of the red AGN have very low cold gas absorbing columns and we term these 'red candidates', i.e. AGN whose nuclear optical continuum slope is very soft and shows no sign of the BBB. Of the remaining objects, three have an $\alpha_{\rm x}$ significantly harder than

0.5 and are probably absorbed.

Red AGN as a class have received little attention relative to their blue counterparts (which are considered the norm). The most popular AGN selection techniques (optical and soft X-ray) will have missed many of them; it has been estimated that perhaps 80 per cent of radio-quiet AGN may have been reddened by dust and are unaccounted for. Thus our interpretation of population studies of AGN from predominantly unabsorbed sources are suspect at best, particularly if dust absorption is *not* closely linked with the orientation of the nucleus.

While possible, compelling, links have been made between red quasars (which are radio-loud) and blazars, our red candidate for which radio data is available is radio-quiet, making such an explanation unlikely in this case, unless this red, 'blazar-like' component has a break between the radio and the optical. For most objects, an excess of soft X-ray (0.5-2 keV) emission above an extrapolation of the optical 'blazar' component is also required.

A very good way of searching for red AGN in the future will be from serendipitous detections of AGN in hard X-rays using deep fields from missions like *XMM* and *AXAF*. The effects of cold gas absorption are greatly reduced at higher X-ray energies than those sampled by, say *ROSAT*, and the vast improvements in throughput and spectral resolution promised by these telescopes, especially by *XMM*, should probe even deeper into the nucleus than was previously possible. If indeed there are many red AGN waiting to be discovered, the notion that 'all AGN are blue' must be relaxed, at least until such studies prove otherwise.

ACKNOWLEDGMENTS

We thank all in the RIXOS team for their work in obtaining and reducing the data. We are especially grateful to Ian McHardy and Niel Brandt for their help and advice; also to the anonymous referee whose report improved the paper. The RIXOS project has received observing time under the International Time Programme offered by the CCI of the Canarian Observatories and has received financial support by the European Commission through the Access to Large-Scale Facilities Activity of the Human Capital and Mobility Programme. This research has made use of data obtained from the UK *ROSAT* Data Archive Centre at the Department of Physics and Astronomy, University of Leicester (LEDAS). We also thank the Royal Society for a grant to purchase equipment essential to the RIXOS project.

REFERENCES

Antonucci R., 1993, Ann. Rev. Astron. Astrophys., 31, 473
Barvainis R., 1993, ApJ, 412, 513
Boyle B. J., Wilkes B. J., Elvis, M., MNRAS, 285, 511
Brandt W. N., Fabian A. C., Pounds K. A., 1996, MNRAS, 278, 326
Brandt W. N., Pounds K. A., Fink H., 1995, MNRAS, 273, L47
Breeveld A. A., Puchnarewicz E. M., 1997, MNRAS, submitted
Bregman J. N., Glassgold A. E., Huggins P. J., Kinney A. L., 1985, ApJ, 291, 505
Cardelli J. A., Clayton G. C., 1991, AJ, 101, 1021
Cardelli J. A., Clayton G. C., Mathis J. S., 1989, ApJ, 345, 245
Comastri A., Setti G., Zamorani G., Elvis M., Wilkes B. J., McDowell J. C., Giommi P., 1992, ApJ, 384, 62
Czerny, B., Elvis, M. 1987, ApJ, 321, 305
Donea A. C., Biermann P. L., 1996, A&A, 316, 43
Edelson R. A., Malkan M. A., 1986, ApJ, 308, 509
Elvis M., Green R. F., Bechtold J., Schmidt M., Neugebauer G., Soifer B. T., Matthews K., Fabbiano G., 1986, ApJ, 310, 291
Elvis M., Fiore F., Mathur S., Wilkes B. L., 1994b, ApJ, 425, 103
Elvis M., Wilkes B., M^{c}Dowell J. C., Green R. F., Bechtold J., Willner S. P., Oey M. S., Polomski E., Cutri R., 1994a, ApJS, 95,1
Francis P. J., Hewett P. C., Foltz C. B., Chaffee F. H., Weymann R. J., Morris S. L., 1991, ApJ, 373, 465
Gioia, I. M., Maccacaro, T., Schild, R. E., Stocke, J. T., Morris, S. L., Henry, J. P., 1990, ApJS, 72, 567
Gorenstein P., 1975, ApJ, 198, 40
Grandi S. A., 1983, ApJ, 591
Kollgard R. I., Feigelson E. D., Laurent-Muehleisen S. A., Spinrad H., Dey A., Brinkmann W., 1995, ApJ, 449, 61
Komossa S., Fink H., 1997, A&A, in press
Krolik J. H., Begelman M. C., 1988, ApJ, 329, 702
Laor A., Draine B. T., 1993, ApJ, 402, 441
Laor A., Fiore F., Elvis M., Wilkes B. J., McDowell J. C., 1997, ApJ, 477, 93
Ledden J. E., O'Dell S. L., 1983, ApJ, 270, 434
Madau, P. 1988, ApJ, 327, 116
Malkan M. A., 1984, in *X-ray and UV Emission from Active Galactic Nuclei*, ed. W. Brinckmann and S. Trumper (MPIfR), 121
McDowell J. C., Elvis M., Wilkes B. J., Willner S. P., Oey M. S., Polomski E., Bechtold J., Green R. F., 1989, ApJ, 345, L13
Mittaz J. P. D. et al. , 1997, MNRAS, submitted
Nandra K., 1991, PhD Thesis, University of Leicester
Neugebauer G., Green R. F., Matthews K., Schmidt M., Soifer B. T., Bennet J,. 1987, ApJS, 63, 615
Pfefferman E. et al. , 1986, Proc. SPIE, 733, 519
Pounds K. A., Done C., Osborne J. P., 1995, 277, L5
Pounds K. A., Nandra K., Stewart G. C., George I. M., Fabian A. C., 1990, Nature, 344, 132
Puchnarewicz E. M., Mason K. O., Romero-Colmenero E., Carrera F. J., Hasinger G., M^{c}Mahon R., Mittaz J. P. D., Page M. J., Carballo R., 1996, MNRAS, 281, 1243 (Paper I)
Puchnarewicz E. M. et al., MNRAS, in press Paper II)
Puchnarewicz E. M., Mason K. O., Siemiginowska A., Pounds K. A., 1995, MNRAS, 276, 20
Rieke G. H., Lebofsky M. J., Kinman T. D., 1979, ApJ, 232, L151
Ryter C., Cesarsky C. J., Audouze J., 1975, ApJ, 198, 103
Sargent W. L., Steidel C. C., Boksenberg A., 1989, ApJS, 69, 703
Stark, A. A., Gammie, C. F., Wilson, R. F., Ball, J., Linke, R. A., Heiles, C., Hurwitz, M., 1992, ApJS, 79, 77
Stocke, J. T., Morris, S. L., Fleming, T. A., Gioia, I. M., Maccacaro, T., Schild, R., Wolter, A., Patrick, H. J., 1991, ApJS, 76, 813
Sun W.-H. Malkan M. A., 1989, ApJ, 346, 68
Tananbaum H., Tucker W., Prestwich A., Remillard R., 1997, ApJ, 476, 83
Turner, T. J., Pounds, K. A., 1989, MNRAS, 240, 833
Ulvestaad J. S., Antonucci R. R. J., 1986, AJ, 92, 6
Walter, R., Fink, H. H., 1993, A& A, 274, 105
Webster R. L., Francis P. J., Peterson B. A., Drinkwater M. J., Masci F. J., 1995, Nature, 375, 469
Wills B. J., Netzer H., Wills D., 1985, ApJ, 288, 94

This paper has been produced using the Royal Astronomical Society/Blackwell Science TEX macros.